FARM EFFICIENCY OF LARGE WIND FARMS: EVALUATION USING LARGE EDDY SIMULATION

Niranjan S. Ghaisas
Center for Turbulence Research
Stanford University
nghaisas@stanford.edu

Aditya S. Ghate
Department of Aeronautics and Astronautics
Stanford University
aditya90@stanford.edu

Sanjiva K. Lele
Department of Aeronautics and Astronautics,
and Center for Turbulence Research, Stanford University
lele@stanford.edu

ABSTRACT

The flow in the fully-developed wind-turbine array boundary layer is simulated using large-eddy simulation. The numerical framework is based on Fourier-spectral discretization in the horizontal and sixth-order compact finite differences in the vertical directions, with turbine forces modeled as actuator drag-disks. The numerical method is validated by reproducing previously published results of the flow in the atmospheric boundary layer (ABL) with and without wind turbines. The turbulent kinetic energy (TKE) budget in wind farms with increasing number of turbines in the streamwise direction is studied. The turbulent transport term is found to be negative above the rotor hub-height and positive below the hub-height, indicating a net transfer of TKE from above the hub-height to the lower half of the rotor region. Consistent with previous studies for an isolated turbine, the magnitudes of the turbulent transport, shear production and the TKE itself are found to increase with increasing number of turbines. An analytical model for the performance of infinitely large wind farms is evaluated using LES. A total of 15 simulations, covering aligned and staggered layouts, differing thrust coefficients, streamwise spacings of turbines and surface roughness heights of the ABL, are considered. The model is found to provide correct trends for the LES data, but is found to consistently under-predict the power and thrust coefficients, by approximately $5-20\%$ and $1-12\%$, respectively. The under-prediction is partly explained by the assumptions of inviscid flow and validity of the classical actuator-disk theory, inherent in the one-dimensional model. The LES results suggest that the empirical parameter employed by the analytical model can be estimated based on the turbine loading.

INTRODUCTION

Large eddy simulations (LES) of an atmospheric boundary layer (ABL) with a large number of wind turbines immersed are carried out. In wind farms where the horizontal length scale over which the turbines are present is at least one order of magnitude larger than the vertical extent of the atmospheric boundary layer, the flow may be assumed to be 'fully-developed' (Meneveau, 2012). A portion of this fully-developed wind farm boundary layer, with a small number of turbines, is simulated by enforcing periodic conditions at the horizontal boundaries.

The temporally and horizontally averaged mean flow in such wind farms is represented fairly accurately by single-column 'top-down' models (Meneveau, 2012) and its variants incorporating effects of lateral expansion of wakes (Yang *et al.*, 2012; Stevens *et al.*, 2015). Previous experimental (Cal *et al.*, 2010) and numerical (Calaf *et al.*, 2010; VerHulst & Meneveau, 2015) investigations of the mean kinetic energy budget in large wind farms have established that the energy extracted by turbines is primarily balanced by the vertical flux of mean kinetic energy due to turbulent fluctuations. The budget of the turbulent kinetic energy (TKE) has been studied for isolated turbines (Wu & Porté-Agel, 2012; Abkar & Porté-Agel, 2015). A similar analysis of the terms in the TKE equation is discussed briefly in this paper.

An analytical model for evaluating the power generated and efficiency of large wind farms was developed recently by Nishino (2016), based on momentum balance arguments and the classical inviscid actuator-disk theory. The model provides a way for determining the performance of wind farms, given the thrust coefficient of the turbines, geometric parameters such as turbine diameter and layout, and characteristics of the undisturbed ABL. Simulations covering a wide range of turbine and atmospheric input parameters are carried out and used for evaluating this analytical model.

The numerical framework and validation of the LES code used for the simulations are discussed first. The budget of the turbulent kinetic energy is studied next, for three aligned wind farms where the thrust coefficient of turbines and surface roughness height kept fixed, and turbine density is varied. In addition, a series of wind farms with aligned and staggered arrangement of turbines, varying number of turbines, turbine thrust coefficients and surface roughness heights, are simulated to test a theoretical model for wind farm efficiency developed by Nishino (2016). Evaluation of the predictions of the theoretical model and the behavior of the free parameter are presented using the LES, followed by the conclusions.

NUMERICAL FRAMEWORK AND VALIDATION

The incompressible LES-filtered Navier-Stokes equations are solved on a Cartesian grid using a recently developed code with Fourier collocation in x and y directions, a sixth-order staggered compact finite-difference scheme in the vertical z direction and a third-order, total variation diminishing Runge-Kutta (TVD-RK3) method for time integration scheme. The Sigma model (Nicoud *et al.*, 2011) is used for sub-grid scale (SGS) closure. A wall model based on Monin-Obukhov Similarity Theory is used to specify the wall shear stress at the bottom boundary to enable simulations at effectively infinite Reynolds numbers. Turbine forces are modeled using a standard actuator-disk approach, with a thrust coefficient C_T' as an input parameter. The wall and turbine models are very similar to those described in Calaf *et al.* (2010). The flow is driven by a constant pressure gradient in the x direction. Statistical averaging is performed over time and horizontal directions (denoted by $\langle..\rangle$), once quasi-stationary conditions are reached.

The code is validated by reproducing the case labeled A2 by Calaf *et al.* (2010). All quantities are non-dimensionalized using the boundary layer height, H, and the friction velocity in the absence of turbines, u_*. The domain is $\pi \times \pi \times 1$, surface roughness height, $z_0/H = 10^{-4}$, and the driving pressure gradient $u_*^2/H = 1$. Typical values of the length and velocity scales are $u_* = 0.45$ m/s, and $H = 1000$ m. All simulations were carried out for over 100 time units (H/u_*), with averaging performed over the last 70 time units. An ABL without wind turbines is simulated first. The mean velocity profile, shown in Fig. 1a, follows the expected logarithmic law-of-the-wall, $u = (u_*/\kappa)\, ln(z/z_0)$, with $\kappa = 0.4$. The total shear stress decreases linearly from 1 at the ground to 0 at the top of the domain (not shown).

Simulation results of a 4×6 array of identical wind turbines with hub-height $z_h/H = 0.1$, rotor-diameter $D/H = 0.1$ and thrust coefficient $C_T' = 4/3$ are conducted. The turbine layout and instantaneous flow features are seen in Fig. 3a. Similar to Calaf *et al.* (2010), two logarithmic profiles are observed outside of the turbine rotor region (Fig. 1a). The lower log-law is described by a modified friction velocity, $u_{*,lo}$, while the upper log-law has a modified roughness height, $z_{0,hi}$. The quantities $[u_{*,lo}, z_0/z_h] = [0.57, 0.032]$ extracted from our LES compare very well with $[0.58, 0.034]$ obtained by Calaf *et al.* (2010).

The shear stress (Fig. 1b), kinetic energy flux and turbulent production (Fig. 1c) profiles using two grid resolutions compare well with the results of Calaf *et al.* (2010). As expected, the magnitude of the SGS terms is seen to reduce with increasing resolution (Fig. 1(b)). In general, the agreement in the rotor region improves with increasing resolution. Since all of the trends and most of the magnitudes compare well with previous results, we may conclude that our numerical method is validated.

Fig. 1(b) and (c) indicate that the simulation results with 64^3 grid points display the same qualitative features as the 128^3 grid results. Although not fully converged, qualitative inferences may be drawn based on simulations on the coarser grid. In view of the large number of simulations needed to explore the parameter space, particularly for the purpose of evaluating the wind farm efficiency model, we restrict the resolution to 64^3 grid points. A total of 14 LES are carried out, with parameters summarized in Tables 1 and 2.

TURBULENT KINETIC ENERGY BUDGET

Previous studies on large wind farms, e.g. Calaf *et al.* (2010); VerHulst & Meneveau (2015), have focused on the budget of the mean kinetic energy, and established that the power extracted by wind turbines is primarily balanced by the vertical flux of mean kinetic energy. The budget of the turbulent kinetic energy (TKE) is analyzed here. The equation governing the resolved TKE, $k = (1/2)\,\overline{u_i' u_i'}$ is

$$\frac{Dk}{Dt} = -\frac{\partial \overline{u_j' k}}{\partial x_j} - \frac{\partial \overline{u_j' p'}}{\partial x_j} - \frac{\partial \overline{u_i' \tau_{sgs,ij}'}}{\partial x_j} - \overline{u_i' u_j'}\frac{\partial \bar{u}_i}{\partial x_j} - \overline{u_i' f_i'} - \overline{\tau_{sgs,ij}' S_{ij}'}. \tag{1}$$

The first, fourth, fifth and sixth terms on the right-hand side of the above equation represent turbulent transport, shear production, wind-turbine work and SGS dissipation, respectively. Horizontally- and time-averaged profiles of these four terms are shown in Fig. 2(a) for LES runs with different turbine densities. Fig. 2(b) shows the corresponding time- and horizontally-averaged TKE profiles. It is clear that the shear production is a source of TKE, while the SGS dissipation and wind-turbine work act as sinks. The turbulent transport term is positive in the lower half of the turbine rotor region ($0.05 \le z \le 0.1$), and negative in the upper half ($0.1 \le z \le 0.15$) of the rotor region. Thus the net effect of the turbulent transport term is to redistribute TKE from above the turbine rotor to regions below the hub-height. All four terms are of similar orders of magnitude, with the shear production being approximately twice as large as the turbulent transport. These trends are seen to hold for farms with turbine densities varying from 4×8 to 4×4. Increasing turbine density leads to increased magnitudes of TKE, consistent with the increased magnitudes of the vertical flux of TKE and the shear production.

EVALUATION OF WIND FARM EFFICIENCY MODEL

A theoretical model for the efficiency of an infinitely large wind farm was developed recently by Nishino (2016). The theory is based on the momentum balance,

$$\langle \tau \rangle_{w0} = \langle \tau \rangle_w + \langle T \rangle_T / S, \tag{2}$$

which states that the sum of forces exerted by the ground and the turbines equals the force exerted by the ground in the absence of turbines. Here, $\langle T \rangle_T$ denotes the time- and turbine-averaged thrust force, S denotes the effective area occupied by each turbine, and $\langle \tau \rangle_w$ and $\langle \tau \rangle_{w0}$ denote the wall shear stresses in the presence and absence of turbines, respectively. This equation was cast into non-dimensional form and in terms of a 'turbine-scale' wind speed reduction factor, $\alpha = U_T/U_F$, and a 'farm-scale' wind speed reduction factor, $\beta = U_F/U_{F0}$, as

$$1 - \beta^\gamma = \frac{\lambda}{C_{f0}} \beta^2 \cdot 4\alpha(1-\alpha). \tag{3}$$

U_T is the disk-averaged velocity, while U_F and U_{F0} are velocities averaged over a 'wind-farm layer' with and without turbines, respectively. $\lambda = \pi D^2/4S$ is the ratio of rotor-disk area to the planform area, and C_{f0} is a friction coefficient in the absence of wind farms. The thrust is assumed

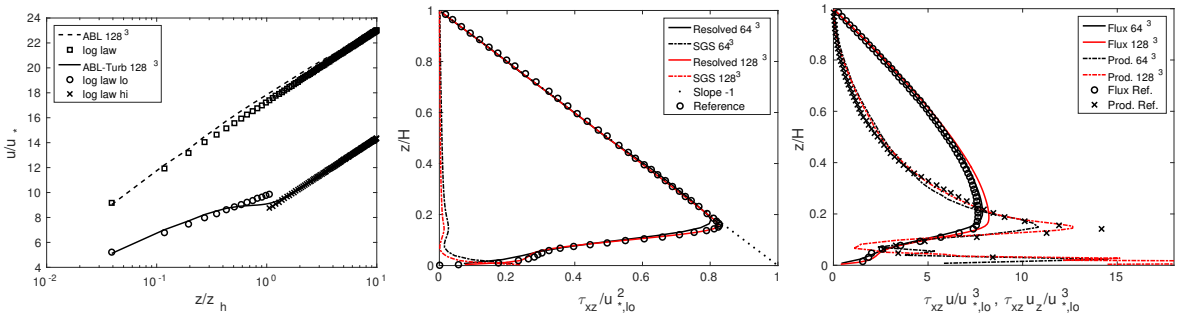

(a) (b) (c)

Figure 1. Comparison of turbulent statistics in ABL with wind turbines with reference results of case A2 reported in Calaf *et al.* (2010). Profiles of (a) mean velocity, (b) shear stress, and (c) kinetic energy flux and turbulent production. Rotor region is $0.05 \leq z \leq 0.15$.

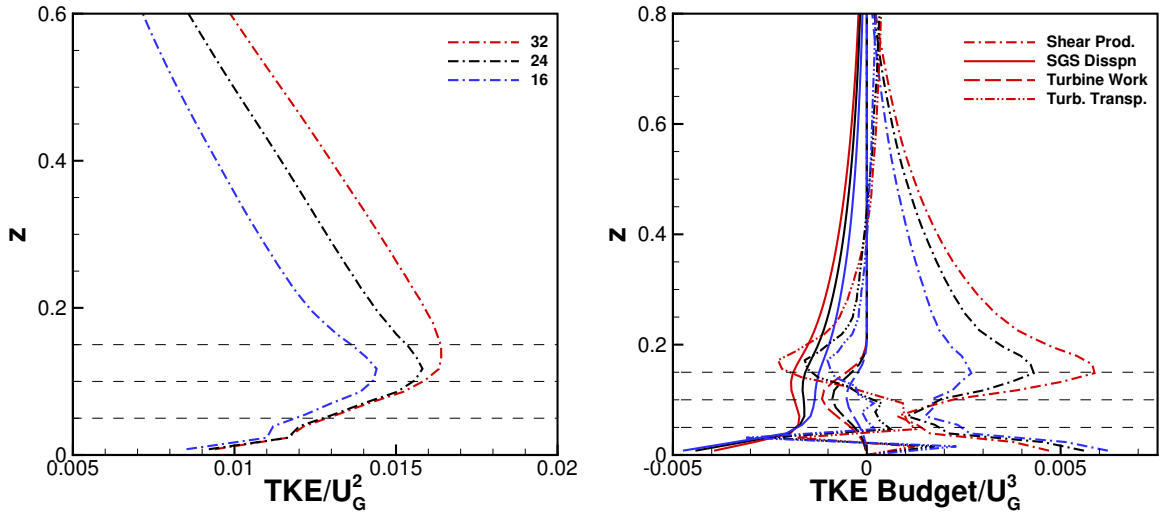

(a) (b)

Figure 2. (a) TKE and (b) terms in the TKE budget equation extracted from LES of wind farms with fixed $C_T' = 4/3$, $z_0 = 10^{-4}$ and varying turbine density. Turbine densities 4×8, 4×6 and 4×4 represented by red, black and blue lines, respectively. Rotor region is $0.05 \leq z \leq 0.15$, denoted by black dashed horizontal lines.

to be given by the classical actuator disk theory. This implies that for a wind farm comprised of turbines with a given C_T', the model assumes a value of $\alpha_{mod} = 4/(C_T' + 4)$. The above definitions allow calculation of thrust and power coefficients, $C_T = 4\beta^2\alpha(1-\alpha)$ and $C_P = 4\beta^3\alpha^2(1-\alpha)$. The model employs an empirical parameter γ, formally defined by the relation

$$\frac{\langle\tau\rangle_{w0}}{\langle\tau\rangle_w} = \left(\frac{U_{F0}}{U_F}\right)^{\gamma}. \tag{4}$$

For the purpose of evaluating the model, several LES are carried out with varying C_T', z_0, turbine streamwise spacing and layout. The spanwise spacing of turbines is always kept fixed at $\pi/4$, so there are four columns of turbines in all farms. The turbine layout and the resulting flow patterns in two of the wind farm configurations are illustrated in the instantaneous snapshots of horizontal velocity contours shown in Fig. 3. The turbine wakes and flow features are seen to be drastically different in the staggered, as compared to the aligned, configuration. Some of the key parameters in the Nishino (2016) model extracted from the LES are summarized in Tables 1 and 2 and in Fig. 4. Cases with a fixed $C_T' = 4/3$ and varying turbine density, surface roughness and layout are included in Table 1. Table 2 lists some cases with fixed layout and surface roughness but varying turbine density for $C_T' = 2$ and 0.5.

The LES runs can be seen to be well converged, since eq. 2 is satisfied accurately. The residual in eq. 2 is seen to be less than 1% in all but one case, with the maximum error about 3%. The values of α extracted from the LES are seen to be consistently higher than α_{mod}. This is expected since the theory assumes that the flow in the turbine wakes is inviscid. On the contrary, in the LES, the turbulent mixing across the turbulent shear layer in the wind turbine wake is expected to lead to larger velocity of the flow through the disk (U_T), and hence, larger α (see Nishino & Wilden (2012)). Comparing the first and last rows in Table 1, it is clear that the mismatch of α is also partly explained by grid resolution, since the results change by about 5% on increasing resolution.

The power and thrust coefficient values obtained from the LES are compared to the model predictions in Fig. 4. Despite the mismatch in the turbine-scale wind speed reduction factors discussed above, the predictions for C_P and C_T are generally good across all the cases evaluated here.

Fig. 4(a) shows that the model predictions are not very sensitive to the value of γ, and vary by only about 5% as γ varies from 1.7 to 2.3. The model predictions are more sensitive to λ/C_{f0} and C_T' than to γ. Model predictions with $\gamma = 2$ alone are shown in Fig. 4(b) to avoid clutter.

The errors in C_P and C_T between the LES and model predictions are quantified in Tables 1 and 2. The model is seen to underpredict C_P by about 5% to 20%, while C_T is underpredicted by a smaller amount. The model predictions used to assess these errors are based on the actual values of γ obtained from the LES. The mismatch between computed and modeled C_P and C_T values can be explained by the fact that, similar to the classical actuator disc theory, the analytical model by Nishino (2016) is valid for a uniform inflow and inviscid flow in the turbine wakes. On the other hand, in the LES, the horizontal and vertical shear upstream of turbines and strong turbulent mixing in the turbine wakes leads to significant differences in the streamwise momentum balance. It was shown in Nishino (2016), that the 1D inviscid theory under-predicted the local thrust coefficient obtained from 3D RANS by approximately 11%, which is consistent with the magnitudes of the under-predictions ofC_P and C_T obtained in our study.

Based on the rationalization that the installation of turbines in an ABL should lead to an increased surface friction coefficient, i.e. $C_f \geq C_{f0}$, Nishino (2016) argued that γ should vary in the range $\gamma \in [1,2]$. The upper bound on γ allowed Nishino (2016) to define a 'maximum efficiency' for large wind farms. Tables 1 and 2 show that γ was found to exceed 2 in several of our LES cases. This suggests that the upper bound on efficiency imposed by the 1D theoretical model may be violated in actual three-dimensional simulations. We note that the only condition implied by the momentum balance on the relation between the two friction coefficients is $C_{f0} \geq C_f \beta^2$. This is obtained by dividing eq. 2 by $(1/2)\rho U_{F0}^2$, and rearranging the resulting equation. Thus, the momentum balance does not restrict γ to be less than 2.

In order for the model to be fully predictive, the value of γ has to be specified. We use the LES data to gain insight into the value of γ. Fig. 5(a) shows the LES data as a scatter plot with $\log(\langle\tau\rangle_w / \langle\tau\rangle_{w0})$ and $\log(U_F/U_{F0})$ on the two axes. Smaller values of $\log(\langle\tau\rangle_w / \langle\tau\rangle_{w0})$ denote wind farms with stronger turbine loading, while larger values imply a weaker turbine loading. A linear least-squares fit with slope of $1/1.8$ is seen to represent the data for stronger turbine loading, while the data for weaker turbine loading is seen to be better represented by a linear fit with slope $1/2.1$. This suggests that different values of γ are appropriate in different regimes of turbine loading. Fig. 5(b) plots γ as a function of $c_{ft}' = \pi C_T'/(4 s_x s_y)$, where $s_x D$ and $s_y D$ are spacings in the x and y directions, respectively. The parameter c_{ft}' is a friction coefficient based on the planform area, S, and has been used in top-down models, e.g. Calaf *et al.* (2010), to quantify turbine loading. Except for one outlier, all cases seem to follow the broad trend of decreasing γ with increasing turbine loading.

SUMMARY AND OUTLOOK

LES of large wind farms have been carried out using a newly developed pseudo-spectral code that employs Fourier-spectral collocation in the horizontal directions, a sixth-order compact scheme in the vertical, and a TVD-RK3 time-stepping scheme. The turbine forces are modelled using an actuator drag-disk model. Results of a baseline ABL simulation without turbines and a simulation comprised of 24 turbines arranged in a 4×6 array with a thrust coefficient $C_T' = 4/3$ are found to be in good agreement with results previously published by Calaf *et al.* (2010).

The importance of several terms in the equation governing the turbulent kinetic energy (TKE) are investigated. In the turbine region, TKE is generated by shear production, while SGS dissipation and turbine work act as sinks of TKE. The turbulent transport term effectively transports TKE from above the rotor region to below the hub-height. The magnitudes of TKE and all terms in the TKE budget increase with increasing turbine density.

The LES results are utilized to evaluate the recently developed wind farm efficiency model of Nishino (2016). Several combinations of turbine layout (i.e. aligned vs staggered), turbine thrust coefficients, surface roughness heights, and turbine densities are considered. The Nishino (2016) model provides an analytical method of estimating the performance of a wind farm, given a geometric parameter λ and the friction coefficient C_{f0} of the ABL in the absence of turbines, with one empirical parameter. The trends of thrust and power coefficients with the parameter $\lambda/C_{[}f0$ are, broadly, well captured by the analytical model for the different values of C_T', z_0 and turbine layouts and densities considered. The Nishino (2016) model consistently underpredicted the C_P and C_T values obtained form LES by about $5-20\%$ and $1-12\%$, respectively. The under-prediction of C_P and C_T are along expected lines, since an inviscid one-dimensional model is being compared to three-dimensional LES results where the flow upstream of turbines is sheared horizontally as well as vertically, and the significant turbulent mixing occurring in wind turbine wakes. The magnitudes of the discrepancies, however, need to be further investigated, particularly, with respect to sensitivity to numerical resolution. Contrary to the rationalization in Nishino (2016), values of γ exceeding 2 are found in some of the LES cases. Finally, the LES results suggest that the appropriate value of γ is sensitive to the turbine loading, and increases with decreasing turbine loading.

Future efforts will focus on evaluating the other terms in the TKE transport equation not computed here, and on closure of the TKE budget. It should be noted that the 2/3 rule used for dealiasing affects different terms in the TKE budget equation to different extents, thus rendering the task of achieving full closure difficult. The reasons for quantitative discrepancies between the LES results and Nishino (2016) model predictions will be further investigated. The implications of the free parameter $\gamma > 2$ found in some of the LES cases on the maximum efficiency of wind farms, and methods for determining the empirical parameter γ will be investigated.

ACKNOWLEDGEMENTS

The authors thank Dr. Takafumi Nishino for fruitful discussions and for access to his conference manuscript. A portion of this work utilized computational resources at Stanford High Performance Computing Center. ASG and SKL acknowledge partial support from the Precourt Institute for Energy and Tomkat Center for Sustainable Energy at Stanford University.

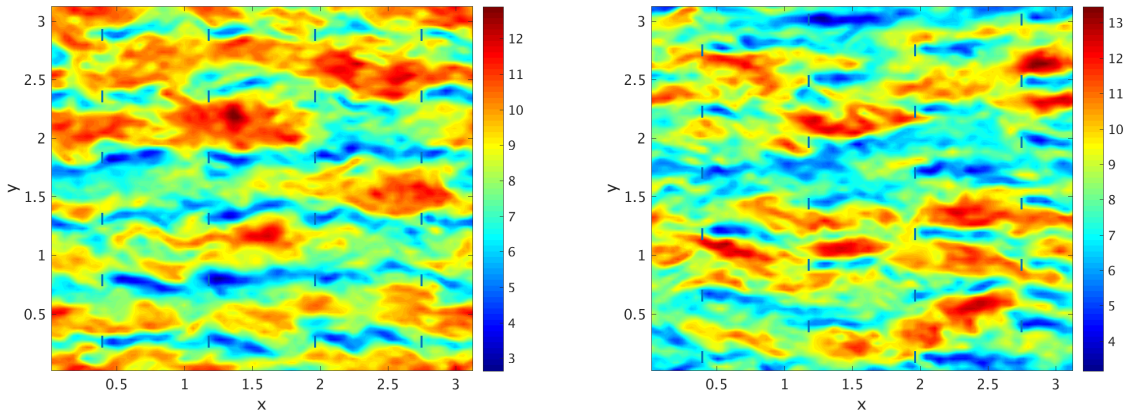

(a) (b)

Figure 3. Instantaneous horizontal velocity contours at hub-height in an (a) aligned and (b) staggered wind farm with spanwise spacing $\pi/6$ using 64^3 grid resolution. Vertical bars represent wind turbines.

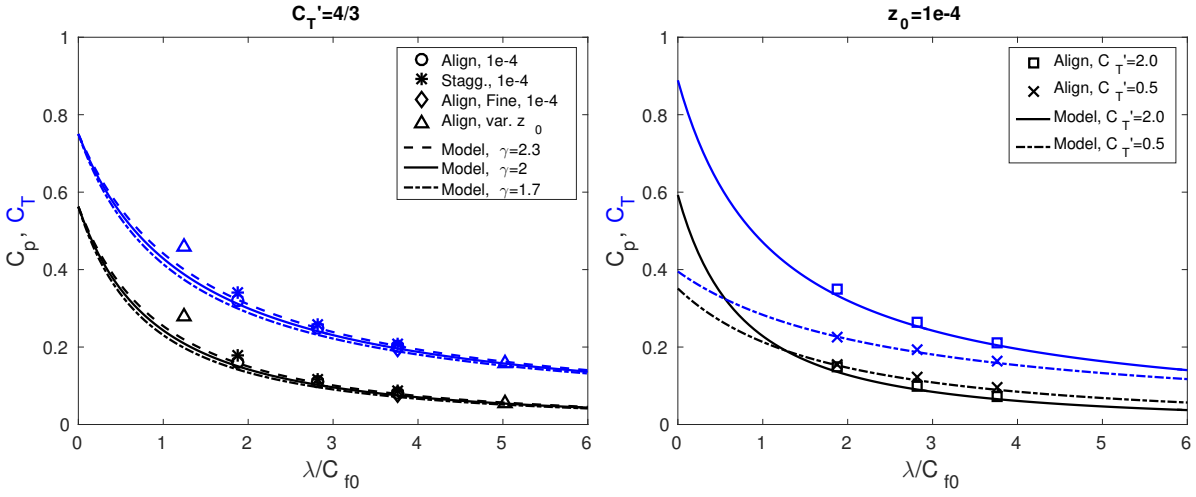

(a) (b)

Figure 4. Comparison of thrust and power coefficients extracted from LES of large wind farms (symbols) with theoretical estimates of Nishino (2016) (lines). (a) Fixed $C_T' = 4/3$, λ/C_{f0} varied by changing turbine density with fixed $z_0 = 10^{-4}$ (stars and circles), and by changing z_0 with fixed turbine density 4×8. (b) Fixed $z_0 = 10^{-4}$, $C_T' = 2$ or 0.5, and λ/C_{f0} varied by changing turbine density.

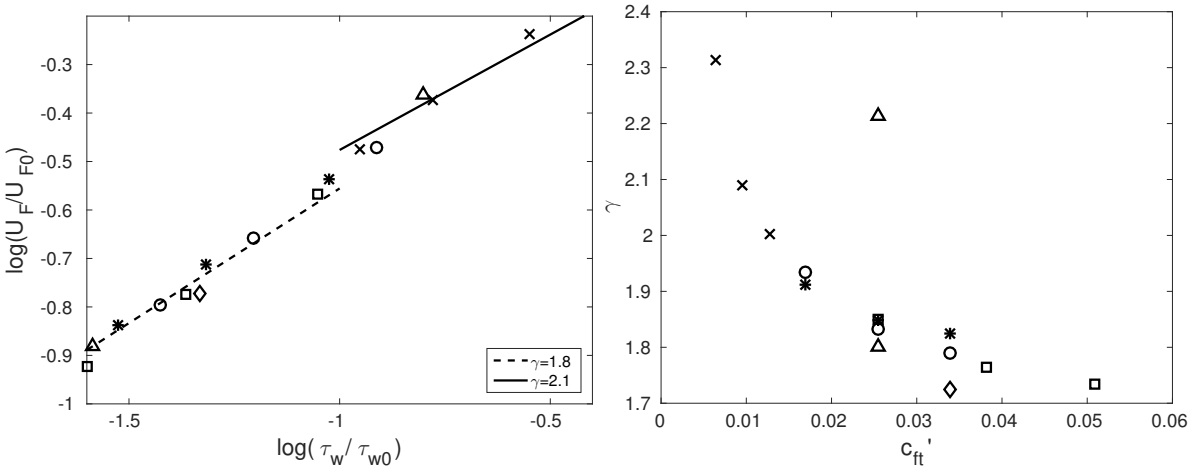

(a) (b)

Figure 5. (a) Scatter plot of quantities extracted from LES data. Lines with slopes 1.8 and 2.1 represent good fits to data for lower and higher values of abscissa. (b) γ as a function of the turbine loading parameter, $c'_{ft} = \pi C_T'/(4 s_x s_y)$, where $s_x D$ and $s_y D$ denote turbine spacings in streamwise and spanwise directions. Legend for symbols is same as in Fig. 4.

Layout	Turb. Density	z_0	Eq. 2 Res. (%)	α	γ	Err. C_P (%)	Err. C_T (%)
Al	4×8	10^{-4}	0.1	0.852	1.79	14.7	7.0
Al	4×6	10^{-4}	0.3	0.826	1.82	13.8	6.9
Al	4×4	10^{-4}	0.6	0.779	1.93	9.2	4.2
St	4×8	10^{-4}	0.1	0.901	1.82	19.4	9.7
St	4×6	10^{-4}	0.1	0.890	1.85	20.4	10.9
St	4×4	10^{-4}	0.2	0.858	1.91	20.9	11.7
Al	4×8	10^{-3}	4.9	0.827	2.22	26.9	14.3
Al	4×4	10^{-3}	0.1	0.825	1.80	9.4	4.4
Al-F	4×8	10^{-4}	0.4	0.819	1.72	10.9	4.8

Table 1. Key parameters in the Nishino (2016) model extracted from LES. $C'_T = 4/3$ for all cases. Eq. 2 Residual is $1 - (\langle\tau\rangle_w + \langle T\rangle_T/S)/\langle\tau\rangle_{w0}$. Case 'Al-F' used 128^3 grid points, all others used 64^3 grid points. Comparison of modelled and computed C_P and C_T are in Fig. 4(a).

Layout	Turb. Density	C'_T	Eq. 2 Res. (%)	α	γ	Err. C_P (%)	Err. C_T (%)
Al	4×8	2	0.2	0.808	1.73	18.1	8.8
Al	4×6	2	0.5	0.780	1.76	18.9	9.6
Al	4×4	2	0.6	0.728	1.85	15.4	7.7
Al	4×8	0.5	0.3	0.914	2.00	7.1	3.1
Al	4×6	0.5	0.3	0.894	2.09	4.4	1.5
Al	4×4	0.5	0.6	0.848	2.31	4.9	4.6

Table 2. Key parameters in the Nishino (2016) model extracted from LES. $z_0 = 10^{-4}$ for all cases. Eq. 2 Residual is $1 - (\langle\tau\rangle_w + \langle T\rangle_T/S)/\langle\tau\rangle_{w0}$. Comparison of modelled and computed C_P and C_T are in Fig. 4(b).

REFERENCES

Abkar, M. & Porté-Agel, F. 2015 Influence of atmospheric stability on wind-turbine wakes: A Large Eddy Simulation study. *Physics of Fluids* **27**, 035104.

Cal, R., Lebron, J., Castillo, L., Kang, H. S. & Meneveau, C. 2010 Experimental study of horizontally averaged flow structure in a model wind-turbine array boundary layer. *Journal of Renewable and Sustainable Energy* **2**, 013106.

Calaf, M., Meneveau, C. & Meyers, J. 2010 Large eddy simulation study of fully developed wind-turbine array boundary layers. *Physics of Fluids* **22**, 015110.

Meneveau, C. 2012 The top-down model of wind farm boundary layers and its applications. *Journal of Turbulence* **13**, 1–12.

Nicoud, F., Toda, H. B., Cabrit, O., Bose, S. & Lee, J. 2011 Using singular values to build a subgrid-scale model for large eddy simulations. *Physics of Fluids* **23**, 085106.

Nishino, T. 2016 Two-scale momentum theory for very large wind farms. *TORQUE 2016, Munich, Germany, October 5-7* pp. 1–10.

Nishino, T. & Wilden, R. H. J. 2012 Effects of 3-D channel blockage and turbulent wake mixing on the limit of power extraction by tidal turbines. *International Journal of Heat and Fluid Flow* **37**, 123–135.

Stevens, R. J. A. M., Gayme, D. & Meneveau, C. 2015 Coupled wake boundary layer model of wind farms. *Journal of Renewable and Sustainable Energy* **7**, 023115.

VerHulst, C. & Meneveau, C. 2015 Altering Kinetic Energy Entrainment in Large Eddy Simulation of Large Wind Farms Using Unconventional Wind Turbine Actuator Forcing. *Energies* **8**, 370–386.

Wu, Y.-T. & Porté-Agel, F. 2012 Atmospheric Turbulence Effects on Wind-Turbine Wakes: An LES Study. *Energies* **5**, 5340–5362.

Yang, X., Kang, S. & Sotiropoulos, F. 2012 Computational study and modeling of turbine spacing effects in infinite aligned wind farms. *Physics of Fluids* **24**, 115107.